Proc. Natl. Acad. Sci. USA
Vol. 91, pp. 3505–3509, April 1994
Neurobiology

Another member of the cyclic nucleotide-gated channel family, expressed in testis, kidney, and heart

(cGMP/ion channel/cloning/calcium)

MARTIN BIEL, XIANGANG ZONG, MADELEINE DISTLER, EVA BOSSE, NORBERT KLUGBAUER, MANABU MURAKAMI, VEIT FLOCKERZI, AND FRANZ HOFMANN*

Institut für Pharmakologie und Toxikologie der Technischen Universität München, Biedersteiner Strasse 29, 80802 Munich, Germany

Communicated by David L. Garbers, December 7, 1993 (received for review August 20, 1993)

ABSTRACT **Cyclic nucleotide-gated cation channels are essential in visual and olfactory signal transduction. An additional member of the cGMP-gated channel family, termed CNG-3, has been cloned from bovine kidney. Its deduced amino acid sequence is 60% and 62% identical with the CNG-channel proteins from bovine rod outer segment and bovine olfactory epithelium, respectively. Northern analysis and sequences amplified by the PCR showed that the CNG-3 mRNA is present in testis, kidney, and heart. Calcium permeated the expressed channel in the presence of extracellular Mg^{2+} and Na^{+} at membrane potentials from −100 to +45 mV. It is likely that CNG-3 protein is responsible for cGMP-induced Ca^{2+} entry in cells other than sensory cells.**

Cyclic GMP is a key regulatory molecule of specific cellular functions such as the visual transduction process (1, 2), relaxation of smooth muscle (3), intestinal secretion of water and salt (4), and reabsorption of Na^{+} and water in the distal tubule of the nephron (5). Overproduction of cGMP has been associated with neuronal degeneration, endotoxin shock, diarrhea, and loss of Na^{+} and water. These diverse cellular effects of cGMP are mediated by several distinct receptors: cGMP-stimulated and -inhibited phosphodiesterases (6), cGMP-dependent protein kinases (3), and cGMP-gated cation channels (1, 2). Cyclic nucleotide-gated (CNG) channels are essential in visual and olfactory signal transduction. These proteins [CNG-1 (7) and CNG-2 (8–10)] are encoded by two different genes. The CNG-1 channel is activated at 40-fold higher cGMP concentrations than the CNG-2 channel. An additional subunit confers high-affinity inhibition by L-*cis*-diltiazem to the rod photoreceptor channel (11). The native and expressed channels are nonspecific cation channels that are highly permeable to monovalent cations and are blocked by the divalent cations Mg^{2+} and Ca^{2+}. In the presence of extracellular Mg^{2+} and Na^{+}, Ca^{2+} permeates these channels at hyperpolarizing membrane potentials (see refs. 1, 2, and 12 for further discussion).

So far, these channels seemed not to be expressed to a significant level in other tissues, although partial sequences of homologous channels have been amplified by PCR from kidney (13) and heart (14). A functional olfactory CNG-2-like channel has been cloned from a rabbit aorta library (10), but its tissue and cellular localization remained unsolved. However, a few reports suggested that cGMP-gated Ca^{2+} entry was mediated by CNG channels in nonsensory cells at depolarized membrane potentials (15–17). Apparently, a cGMP-gated channel mediated Ca^{2+} entry in calcium-depleted pancreatic acinar cells (15). Cultured renal epithelial A6 cells have a cGMP-stimulated cation-channel activity (16). Atrio-natriuretic factor, which stimulates cGMP production in the kidney, increased glomerular filtration by relaxation of preglomerular arterioles and contraction of postglomerular arterioles (17, 18). This communication supports these reports and shows that bovine kidney expresses another member of the CNG-channel family, one which is permeable to Ca^{2+} at a wide range of membrane potentials.†

METHODS

Cloning Strategy. Two degenerate oligonucleotide primers (primer 1: 5′-CGGGAATTCTGGTTYGAYTAYYTGTGG-ACNAAYAA-3′; primer 2: 5′-CGGGAATTCGCYTCCAT-RAGRTCRTCYTT-3′) were synthesized on the basis of the amino acid sequence of two conserved regions in CNG-1 and CNG-2 [W^{435}FDYLWTNK and K^{576}DDLMEA, numbering amino acid residues corresponding to CNG-1 (7)]. These primers were used to amplify cDNA from bovine kidney by the PCR. Reaction conditions were as described (10). Amplified DNA was digested with *Eco*RI, purified by gel electrophoresis, and subcloned into pBluescript (Stratagene). Seventeen clones were analyzed by restriction analysis and sequencing. One clone (pCGK7) was obtained with a 443-bp insert that was identical to the sequence of CNG-1. Sixteen clones contained a 443-bp insert that had 91% amino acid sequence identity and 73% nucleotide sequence identity to CNG-1. Screening of a directional, oligo(dT)-primed bovine kidney cDNA library constructed in the pSPORT1 vector (GIBCO/BRL) with the ^{32}P-labeled insert of one of these clones (pCGK5) yielded two clones, pCGK25 and pCGK26. The sequence shown derives from clone pCGK26 [3954 bp, excluding the poly(A) tail], which was fully sequenced on both strands using either ^{35}S-labeled dATP or a laser fluorescence DNA sequencer.

Transfection of Human Embryonic Kidney 293 Cells. Recombinant plasmids pCGK26/CMV and pCG357/CMV were used for transient expression (19) of CNG-3 and of the rabbit aorta CNG (rACNG) channel (10), in human embryonic kidney 293 cells. These cells do not express endogenous CNG channels (8). pCGK26/CMV was constructed as follows: PCR was done with pCGK26 as template and the following primers: a 5′ adapter primer containing a *Hin*dIII restriction site followed by a consensus sequence for initiation of translation in vertebrates and the first 20 nt from the coding region of pCGK26 and a gene-specific 3′ primer. The PCR product was digested with *Hin*dIII and *Bgl* II to yield an 83-bp fragment. The 83-bp fragment and the 2.2-kb *Bgl* II–*Xba* I fragment from pCGK26 were ligated with the *Hin*dIII–*Xba* I fragment from the pRC/CMV vector (Invitrogen), yielding pCGK26/CMV. The recombinant plasmid

The publication costs of this article were defrayed in part by page charge payment. This article must therefore be hereby marked "*advertisement*" in accordance with 18 U.S.C. §1734 solely to indicate this fact.

Abbreviations: CNG, cyclic nucleotide-gated; rACNG, rabbit aorta CNG.

*To whom reprint requests should be addressed.

†The sequence reported in this paper has been deposited in the GenBank data base (accession no. X76485).

pCG357/CMV was constructed by subcloning the cDNA insert of pCG357 (10) into the *Hin*dIII site of pRC/CMV.

Northern Analysis. Poly(A)$^+$ RNA was prepared from rabbit ileum, aorta, and brain and bovine tongue, cardiac atrium, cardiac ventricle, renal cortex, renal medulla, and testis. Ten micrograms each was separated on a 1.2% agarose gel, transferred to Biodyne nylon membranes (Pall), and hybridized as described (20). The probe used was the ^{32}P-labeled *Eco*RI (913)–*Eco*RI (2199) fragment derived from pCGK26.

Electrophysiology. Patch-clamp recordings were made 2–4 days after transfection by using inside–out patches and the whole-cell recording mode (21). The following solutions were used: solution A, 10 mM glucose/140 mM NaCl/5 mM KCl/10 mM NaHepes/0.5 mM NaEGTA/0.5 mM NaEDTA (pH 7.2); solution B, 10 mM glucose/140 mM NaCl/5 mM KCl/10 mM NaHepes (pH 7.2); solution C, 140 mM potassium aspartate, 8 mM NaCl/10 mM EGTA/10 mM NaHepes (pH 7.2); solution D, 140 mM NaCl/2.8 mM KCl/10 mM $CaCl_2$/2 mM $MgCl_2$/10 mM NaHepes (pH 7.2).

RESULTS AND DISCUSSION

Two degenerate oligodeoxynucleotide primers designed after highly conserved peptide sequences in bovine CNG cation channels, CNG-1 (7) and CNG-2 (9), were used in a PCR to amplify homologous sequences from bovine kidney cDNA. PCR clones obtained could be assigned to two classes. One of the clones (pCGK7) was identical to the sequence of CNG-1. Clones of the other class showed 91% amino acid identity and 73% nucleotide sequence identity to CNG-1, indicating that these sequences potentially represented an additional CNG channel, referred to as CNG-3. To obtain a full-length clone of CNG-3 one of these clones (pCGK5) was used to screen a cDNA library from bovine kidney. Two clones were identified, the largest of which (pCGK26) was fully sequenced. The longest open reading frame encodes a 706-aa protein of calculated M_r^+ 81,132 with a putative transmembrane topology similar to that of related CNG channels (Fig. 1). Amino acid-sequence comparison reveals an overall sequence identity of 60% to CNG-1 and 62% to CNG-2. The largest divergence occurs at the amino-terminal region preceding the first putative transmembrane domain.

The electrophysiological properties of CNG-3 were investigated by using inside–out patches excised from human embryonic kidney 293 cells transfected with a eukaryotic expression vector containing CNG-3-specific cDNA (Fig. 2). The CNG-3 channel was compared with rACNG channel (10), which has been cloned from rabbit aorta and is an olfactory-like channel. cGMP and cAMP activated both channels at positive and negative membrane potentials. cAMP induced 80% and 100% of the maximal current observed in the presence of cGMP in cells expressing CNG-3 and rACNG channels, respectively. In control experiments a total of 25 patches were excised from nontransfected cells; none of these responded to cyclic nucleotides. The apparent K_a values of CNG-3 for cGMP (18 μM at +40 mV) and cAMP (1.9 mM at +40 mV) (Fig. 2*b* and Table 1) are similar to those reported for CNG-1 (23). The difference in affinity between cGMP and cAMP is slightly larger for CNG-3 (100-fold) than for CNG-1 (40-fold). cGMP activated both channels with an apparent Hill coefficient of ≈2 (Table 1). In contrast, cAMP activated the CNG-3 channel with an apparent Hill coefficient of 4 or even higher, suggesting that the channel is composed of five identical subunits (2). The apparent K_a values and Hill coefficients of rACNG channel are similar to those determined in *Xenopus* oocytes injected with rACNG channel-specific cRNA (10), indicating that the different affinities of CNG-3 and rACNG channel for cGMP and cAMP

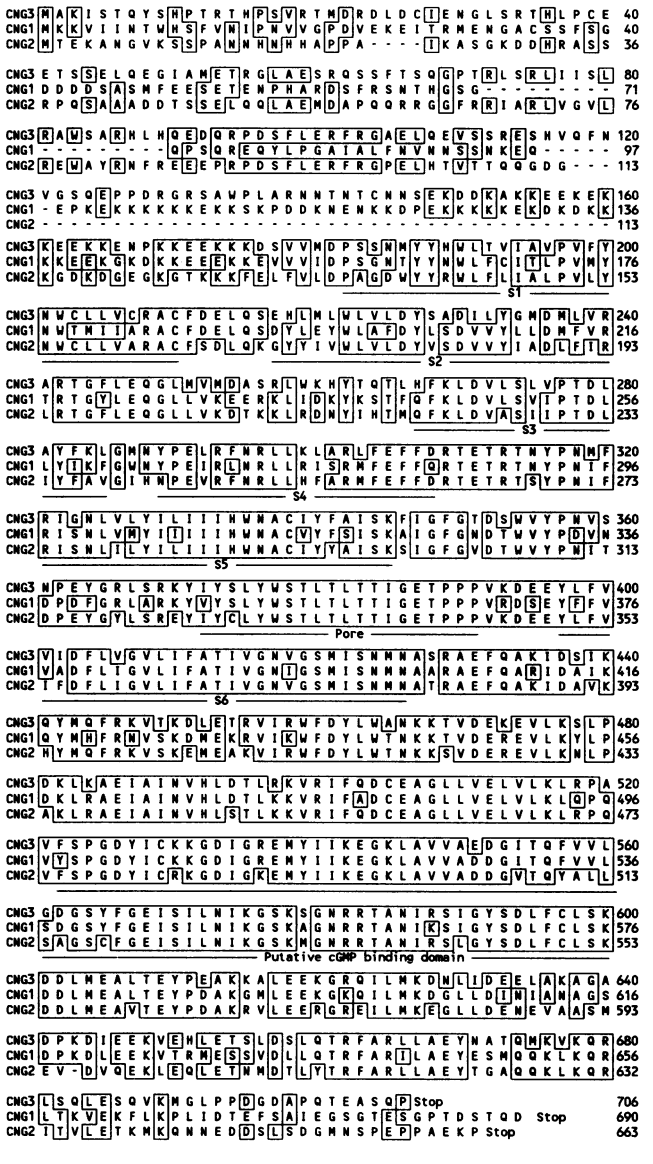

FIG. 1. Primary structure of renal cGMP-gated channel CNG-3. The amino acid sequence of CNG-3 was aligned with that of bovine rod photoreceptor channel CNG-1 (7) and bovine olfactory channel CNG-2 (9). Regions of sequence identity are enclosed in boxes. Gaps in the sequence are represented by dashes. Putative transmembrane domains, the putative pore-forming hairpin (22), and the putative cGMP-binding domain (2) are underlined.

are not determined by the expression system but are intrinsic properties of each channel.

The ion selectivity of CNG-3 was examined by measuring the reversal potential under symmetrical biionic conditions (Fig. 3*a*). On the basis of the Goldman–Hodgkin–Katz equation, permeability ratios P_i/P_{Na} yielded the following series of ion selectivity (n = 6): NH_4^+:Na^+:K^+:Li^+:Rb^+:Cs^+ = 2.32:1.0:0.93:0.91:0.62:0.34. These values are similar to those found with other CNG channels (1, 8–11, 24). CNG-3 showed outward rectification when the divalent cations Mg^{2+} and Ca^{2+} were present in the pipette solution (Fig. 3 *b* and *c*), reflecting the known (see refs. 1, 2, 12) voltage-dependent block of Na^+ conductance. The blocking effect was more pronounced in the presence of 1 mM Mg^{2+} than in the presence of 2 mM Ca^{2+} (Fig. 3*b*). The reversal potential in the presence of 1 mM Mg^{2+} and 2 mM Ca^{2+} ranged between +6 mV and +15 mV. In five experiments, 100 μM L-*cis*-diltiazem blocked the current only by 16.8 ± 2.0%.

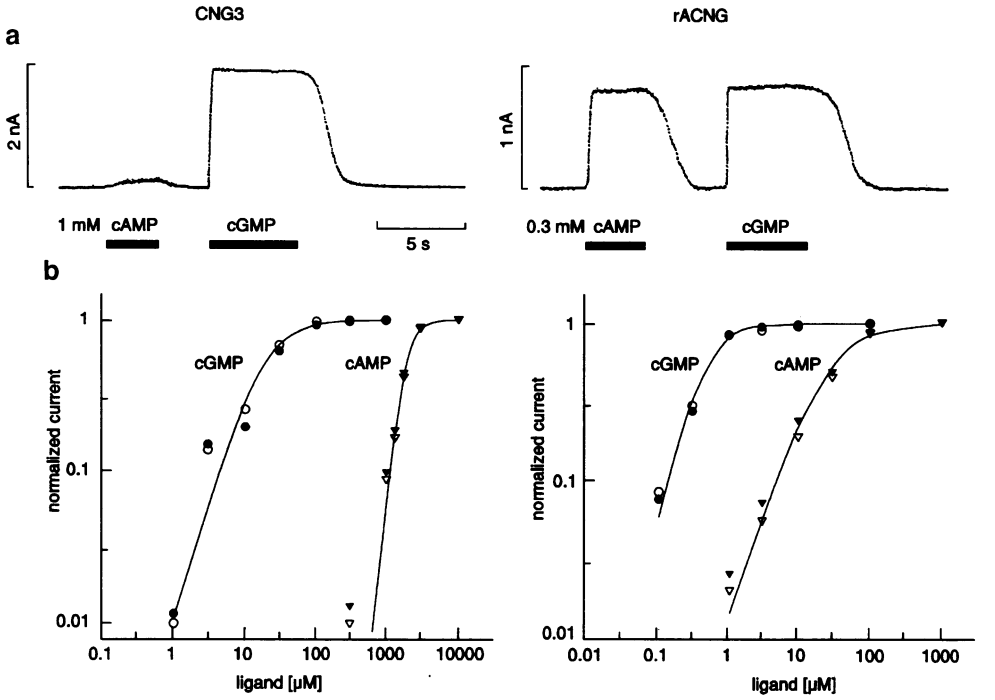

FIG. 2. Comparison between CNG channels produced by the expression of the CNG-3 and the rabbit aorta CNG (rACNG) channel. All results were obtained from inside–out patches of plasma membranes excised from human embryonic kidney 293 cells transfected with the respective cDNA. Solution A was present on both sides of the patch. (*a*) Membrane currents induced by 1 mM cAMP or cGMP (CNG-3) and 0.3 mM cAMP or cGMP (rACNG) in the absence of divalent cations. The membrane potential was +40 mV. (*b*) Normalized dose–response relations between activated current and ligand concentration for cGMP and cAMP. ○ and △, +40 mV; ● and ▲, −40 mV. Each point represents the mean response for 10 (CNG-3, *Left*) and 9 (rACNG, *Right*) patches normalized by the maximal current (I_{max}) obtained at saturating concentrations of cGMP (1 mM for CNG-3 and 100 μM for rACNG) and cAMP (10 mM for CNG-3 and 1 mM for rACNG). The solid lines are the best fit to the open symbols and are scalings of the Hill equation (values given in Table 1): $I/I_{max} = [C]^{\nu}/([C]^{\nu} + K_a^{\nu})$, where $[C]$ is the cyclic nucleotide concentration, K_a is the activation constant, and ν is the Hill coefficient. SEMs were smaller than symbols.

As stated above CNG channels have been implicated in the mediation of Ca^{2+} entry in Ca^{2+}-depleted cells at high membrane potentials (15). Furthermore it has been shown that the photoreceptor (1) and the olfactory channel (25) are permeable to Ca^{2+}. To test this hypothesis, cGMP-activated currents were measured under the ionic conditions used to measure the Ca^{2+} current in Ca^{2+}-depleted cells (26)—i.e., in the presence of 2 and 10 mM extracellular Mg^{2+} and Ca^{2+}, respectively. Under these conditions, cGMP induced an inward current at 0 mV in an excised inside–out patch (Fig. 3*c*), which was not observed in the absence of divalent cations. The current at negative and positive potentials had a significantly decreased amplitude compared with the current in the absence of divalent ions and showed outward rectification. The reversal potential of the current was +45 mV (range: +37 to +58 mV, four experiments), being consistent with the theoretical reversal potential of +47 mV for these ionic conditions (27). This finding suggests that the current was carried, at least in part, by Ca^{2+}. The calculated permeability ratio $P_{Ca^{2+}}/P_{Na^+}$ at 0 mV according to Lewis (27) was 23.6, being in line with Ca^{2+} permeabilities determined for photoreceptor channels (1, 28).

To verify the significance of this inward current, similar experiments were done in the whole-cell configuration. CNG-3-expressing cells were dialyzed with 1 mM cGMP in the absence and presence of Ca^{2+} and Mg^{2+} (Fig. 4*a*). The cells were initially superfused for 1 min with a Ca^{2+}-free solution. Under these conditions, no inward current could be detected while the membrane potential was clamped to 0 mV. Exchange of the Ca^{2+}-free solution by a solution containing 2 and 10 mM extracellular Mg^{2+} and Ca^{2+}, respectively, resulted in a sustained inward current at 0 mV that was reversibly blocked by extracellular Mn^{2+} (10 mM). A symmetrical, linear current–voltage relation was obtained in the absence of divalent cations (data not shown). The divalent cations Mg^{2+} and Ca^{2+} induced an outward rectifying current (Fig. 4 *b* and *d*). Replacement of Ca^{2+} by Mn^{2+} completely blocked the inward current as inferred from the absence of an inward current at 0 mV (Fig. 4 *b* and *d*). The inward current observed at negative membrane potentials was small in comparison with the current in the absence of Mn^{2+}. Nontransfected cells dialyzed with 1 mM cGMP had a small linear current that showed no rectification (Fig. 4 *c* and *d*). A similar current was observed in nontransfected cells in the absence

Table 1. Apparent K_a values and Hill coefficients (ν) of currents activated by cGMP and cAMP at membrane potentials (V_m) of +40 mV and −40 mV

			cGMP		cAMP	
	n	V_m, mV	K_a, μM	ν	K_a, μM	ν
CNG-3	10	+40	18.00 ± 1.62	1.56 ± 0.20	1920 ± 24.9	4.24 ± 0.20
		−40	21.70 ± 2.33	1.52 ± 0.22	1860 ± 28.1	4.28 ± 0.25
rACNG	9	+40	0.45 ± 0.04	1.84 ± 0.24	31.80 ± 1.68	1.38 ± 0.09
		−40	0.46 ± 0.02	2.03 ± 0.15	27.50 ± 1.94	1.27 ± 0.11

Entries are means ± SEMs; n, number of experiments.

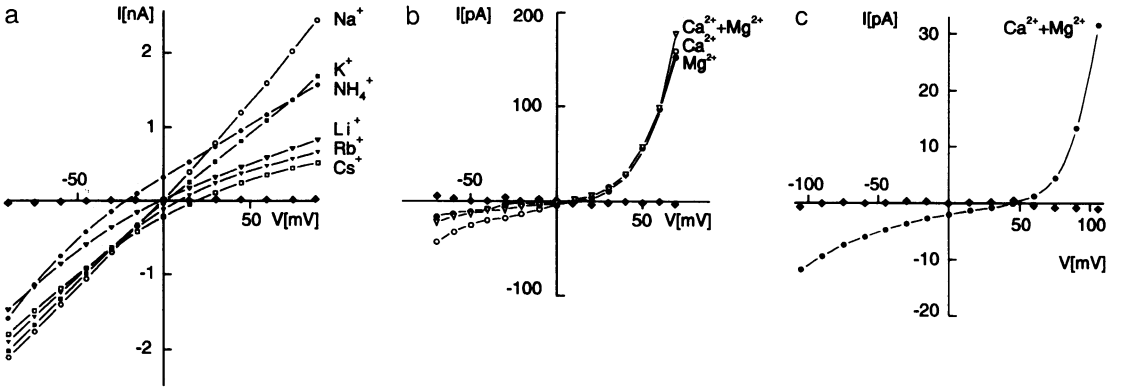

FIG. 3. Steady-state current–voltage relations of CNG-3 under different ionic conditions determined in excised inside–out patches. In all three cases 1 mM cGMP was present in the superfusion solution, which fully saturated the current. Voltage pulses of 400 msec were made at ±15-mV (*a*, *c*) or ± 10-mV (*b*) increments from a holding potential of 0 mV. The current induced at each voltage was measured at the end of the voltage pulse. ◆, Current measured in the absence of cGMP. (*a*) Relations obtained under symmetrical biionic conditions. The patch pipette contained solution A, and the superfusion solution contained the respective cation at 140 mM instead of NaCl in solution A. (*b*) Relations in the presence of 1 mM Mg^{2+} (●), 2 mM Ca^{2+} (○), and both 1 mM Mg^{2+} and 2 mM Ca^{2+} (▽) at the extracellular side. The bath solution contained solution A; the pipette contained solution B supplemented with divalent cations as indicated. (*c*) Relation in the presence of 2 mM Mg^{2+} and 10 mM Ca^{2+} at the extracellular side. The bath and the pipette contained solution C and D, respectively.

of cGMP. The maximal inward current of nontransfected cells measured at −90 mV ranged from −30 to −90 pA (n = 5). In transfected cells the maximal inward current at −90 mV ranged from −700 to −2400 pA and from −60 to −440 pA in the presence of 10 mM Ca^{2+} (n = 9) and 10 mM Mn^{2+} (n = 9), respectively. The current–voltage relation of the Ca^{2+} current (Fig. 4*d*) is very similar to that obtained in the inside–out patch and suggests that the inward current was carried, at least in part, by Ca^{2+}. In addition, the voltage dependence of the Ca^{2+} current is very similar to that reported by Bahnson and colleagues (15). Both currents are outward rectifying. The reversal potential of the current

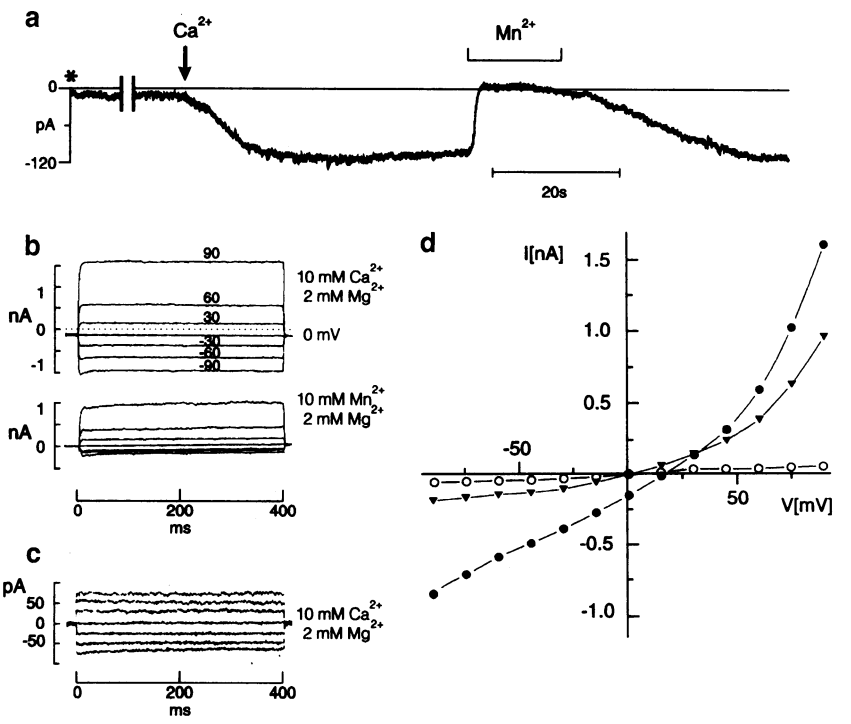

FIG. 4. Permeability of CNG-3 for Ca^{2+} determined in whole-cell configuration. Before cells were used for whole-cell measurement inside–out patches were tested for expression of CNG-3. Serial resistance was compensated as much as possible (>60%). Leak current has not been subtracted. (*a*) Whole-cell current recorded at a holding potential of 0 mV. After an initial superfusion for 1 min with Ca^{2+}-free solution (solution A) the cell was superfused with solution D containing 10 mM $CaCl_2$ and 2 mM $MgCl_2$. The current trace in the absence of Ca^{2+} is only partially shown. Beginning of superfusion with solution D is indicated by an arrow. The pipette contained solution C supplemented with 1 mM cGMP. Establishment of the whole-cell mode is indicated by an asterisk. Solution D with 10 mM $MnCl_2$ instead of $CaCl_2$ was superfused for the time indicated by the horizontal line. Cell capacitance was 35 pF. (*b*) Currents obtained with the same cell as in *a* using voltage steps at increments of ±15 mV from a holding potential of 0 mV in the presence of divalent cations (solution D or solution D with 10 mM $MnCl_2$ instead of $CaCl_2$, as indicated). The pipette contained solution C supplemented with 1 mM cGMP. Only current traces obtained at −90 mV, −60 mV, −30 mV, 0 mV, +30 mV, +60 mV, and +90 mV are shown. (*c*) Currents of a nontransfected cell (cell capacitance = 42 pF) in the presence of divalent cations on the extracellular site as indicated. The pipette contained solution C supplemented with 1 mM cGMP, and the bath contained solution D. Voltage pulses were as described in *b*. (*d*) Current–voltage relation of the currents shown in *b* (●, 10 mM Ca^{2+} and 2 mM Mg^{2+}; ▼, 10 mM Mn^{2+} and 2 mM Mg^{2+}) and *c* (○).

determined in whole-cell configuration is slightly less positive than that of the cGMP-stimulated current of acinar cells (+45 mV), reflecting the property of CNG-3 to be permeable for monovalent and divalent cations.

The tissue distribution of the mRNA encoding CNG-3 was determined by Northern analysis (Fig. 5). A major mRNA species of 4.2 kb is predominantly expressed in testis and kidney cortex and medulla. A weak signal was also found in cardiac atrium and ventricle. The mRNA species found in testis and heart are derived from the same gene as that encoding CNG-3 because partial sequences identical with CNG-3 could be amplified by PCR from the mRNA of these tissues (data not shown). No positive signals were seen with mRNA from ileum, tongue, aorta, cerebellum, and total brain. A smaller transcript of 3.0 kb was detected in kidney and testis and may represent a polyadenylylation variant of the CNG-3 transcript.

In addition to CNG-3, a sequence has been amplified by PCR from kidney that is identical with CNG-1. However, the predominant species of bovine kidney appears to be CNG-3 because CNG-3 and CNG-1 were amplified in a 16:1 ratio. Previously, sequences of the rod photoreceptor channel have been identified in mouse cortical collecting-duct cells and rat kidney (13).

Under physiological conditions, CNG-3 should be activated selectively by cGMP. Its electrophysiological properties are similar to those reported for the retinal CNG-1 channel (7, 23), although CNG-3 shows a similar overall homology to both the photoreceptor and olfactory channels. CNG-3 may allow Ca^{2+} permeation not only at negative but also at positive membrane potentials. However, CNG-3 is not responsible for I_{CRAC} [calcium release-activated calcium current (26, 29)] or similar currents (30, 31) because these currents are not activated by cGMP.

The potential physiological role of CNG-3 in testis, kidney, and heart is probably related to the regulation of cellular calcium at a wide range of membrane potentials. CNG-3 could represent the equivalent of a receptor-operated Ca^{2+} channel, which allows neurotransmitter-controlled Ca^{2+} entry. Chemotaxis of sperm cells may be controlled during fertilization by a mechanism similar to olfactory signal transduction because testis expresses members of the olfactory-receptor gene family (32). Sea urchin sperm has a membrane-bound guanylate cyclase that is activated by resact and speract and mediates chemotaxis of the sperm (33). The strong expression of CNG-3 in testis favors the idea that the chemotactic movement of the sperm may be mediated by the cGMP-activated channel. Regardless of the mechanism by which CNG-3 protein increases cytosolic Ca^{2+}—i.e., by allowing Ca^{2+} permeation at hyperpolarizing or depolarizing voltages or by Na^{+}-induced depolarization and opening of voltage-dependent Ca^{2+} channels, its identification as a component of nonsensory cells is important because it indicates that some of the effects of NO and atrio-natriuretic factor may be mediated by an increase and not a decrease (for further review, see refs. 34–36) in cellular Ca^{2+}.

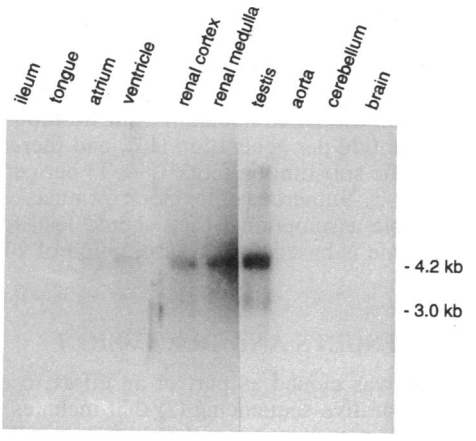

FIG. 5. Northern analysis of CNG-3 expression. Ten micrograms of poly(A)$^{+}$ RNA of each tissue was used. Autoradiographic exposure was 1 day for testis, aorta, cerebellum, and brain and 3 days for ileum, tongue, atrium, ventricle, renal cortex, and renal medulla. No signal was observed in aorta, cerebellum, brain, ileum, and tongue even after an exposure for 7 days.

This work was supported by grants from Deutsche Forschungsgemeinschaft and Fond der Chemie to V.F. and F.H.

1. Yau, K.-W. & Baylor, D. A. (1989) *Annu. Rev. Neurosci.* **12**, 289–327.
2. Kaupp, U. B. & Koch, K.-W. (1992) *Annu. Rev. Physiol.* **54**, 153–175.
3. Hofmann, F., Dostmann, W., Keilbach, A., Landgraf, W. & Ruth, P. (1992) *Biochim. Biophys. Acta* **1135**, 51–60.
4. Rao, M. C. & Field, M. (1984) *Biochem. Soc. Trans.* **12**, 177–183.
5. Ballermann, B. J. & Brenner, B. M. (1986) *Circ. Res.* **58**, 619–630.
6. Beavo, J. A. & Reifsnyder, D. H. (1990) *Trends Pharmacol. Sci.* **11**, 150–155.
7. Kaupp, U. B., Niidome, T., Tanabe, T., Terada, S., Bönigk, W., Stühmer, W., Cook, N. J., Kangawa, K., Matsuo, H., Hirose, T., Miyata, T. & Numa, S. (1989) *Nature (London)* **342**, 762–766.
8. Dhallan, R. S., Yau, K., Schrader, K. A. & Reed, R. R. (1990) *Nature (London)* **347**, 184–187.
9. Ludwig, J., Margalit, T., Eismann, E., Lancet, D. & Kaupp, U. B. (1990) *FEBS Lett.* **270**, 24–29.
10. Biel, M., Altenhofen, W., Hullin, R., Ludwig, J., Freichel, M., Flockerzi, V., Dascal, N., Kaupp, U. B. & Hofmann, F. (1993) *FEBS Lett.* **329**, 134–148.
11. Chen, T.-Y., Peng, Y.-W., Dhallan, R. S., Ahamed, B., Reed, R. R. & Yau, K.-W. (1993) *Nature (London)* **362**, 764–767.
12. Firestein, S. (1992) *Curr. Opin. Neurobiol.* **2**, 444–448.
13. Ahmad, I., Korbmacher, C., Segal, A. S., Cheung, P., Boulpaep, E. L. & Barnstable, C. J. (1992) *Proc. Natl. Acad. Sci. USA* **89**, 10262–10266.
14. Ruiz, M. L., London, B., Logothetis, D. & Nadal-Ginard, B. (1993) *Biophys. J.* **64**, A208 (abstr.).
15. Bahnson, T. D., Pandol, S. J. & Dionne, V. E. (1993) *J. Biol. Chem.* **268**, 10808–10812.
16. Marunaka, Y., Ohara, A., Matsumoto, P. & Eaton, D. C. (1991) *Biochim. Biophys. Acta* **1070**, 152–156.
17. Marin-Grez, M., Fleming, J. T. & Steinhausen, M. (1986) *Nature (London)* **324**, 473–476.
18. Lanese, D. M., Yuan, B. H., Falk, S. A. & Conger, J. D. (1991) *Am. J. Physiol.* **261**, F1102–F1109.
19. Ausubel, F. M. & Frederick, M., eds. (1989) *Current Protocols in Molecular Biology* (Greene and Wiley Interscience, New York), pp. 9.1.3–9.1.4.
20. Hullin, R., Singer-Lahat, D., Freichel, M., Biel, M., Dascal, N., Hofmann, F. & Flockerzi, V. (1992) *EMBO J.* **11**, 885–890.
21. Hamill, O. P., Marty, E., Neher, E., Sakmann, B. & Sigworth, F. J. (1981) *Pflügers Arch.* **391**, 85–100.
22. Guy, R. H., Durell, S. R., Warmke, J., Drysdale, R. & Ganetzky, B. (1991) *Science* **254**, 730.
23. Altenhofen, W., Ludwig, J., Eismann, E., Kraus, W., Bönigk, W. & Kaupp, U. B. (1991) *Proc. Natl. Acad. Sci. USA* **88**, 9868–9872.
24. Frings, S., Lynch, J. W. & Lindemann, B. (1992) *J. Gen. Physiol.* **100**, 45–67.
25. Zufall, F. & Firestein, S. (1993) *J. Neurophysiol.* **69**, 1758–1768.
26. Hoth, M. & Penner, R. (1992) *Nature (London)* **355**, 353–355.
27. Lewis, C. A. (1979) *J. Physiol. (London)* **386**, 417–445.
28. Menini, A., Rispoli, G. & Torre, V. (1988) *J. Physiol. (London)* **402**, 279–300.
29. Penner, R., Fasolato, C. & Hoth, M. (1993) *Curr. Opin. Neurobiol.* **3**, 368–374.
30. Randriamampita, C. & Tsien, R. Y. (1993) *Nature (London)* **364**, 809–814.
31. Parekh, A. B., Terlau, H. & Stühmer, W. (1993) *Nature (London)* **364**, 814–818.
32. Parmentier, M., Libert, F., Schurmans, S., Schiffmann, S., Lefort, A., Eggerickx, D., Ledent, C., Mollereau, C., Gérard, C., Perret, J., Grootegoed, A. & Vassart, G. (1992) *Nature (London)* **335**, 453–455.
33. Garbers, D. L. (1989) *Annu. Rev. Biochem.* **58**, 719–742.
34. Ahlner, J., Andersson, R. G. G., Torfgard, K. & Axelsson, K. (1991) *Pharmacol. Rev.* **43**, 351–409.
35. Lincoln, T. M. & Cornwell, T. L. (1993) *FASEB J.* **7**, 328–338.
36. Walter, U. (1989) *Rev. Physiol. Biochem. Pharmacol.* **113**, 41–88.